Published online 11 June 2022

Nucleic Acids Research, 2022, Vol. 50, No. 11 ***6251–6263***
https://doi.org/10.1093/nar/gkac491

Noncanonical NF-κB factor p100/p52 regulates homologous recombination and modulates sensitivity to DNA-damaging therapy

Brian Budke, Alison Zhong, Katherine Sullivan, Chanyoung Park, David I. Gittin, Timothy S. Kountz and Philip P. Connell*

Department of Radiation and Cellular Oncology, University of Chicago, Chicago, IL, USA

Received April 13, 2020; Revised May 17, 2022; Editorial Decision May 23, 2022; Accepted May 25, 2022

ABSTRACT

Homologous recombination (HR) serves multiple roles in DNA repair that are essential for maintaining genomic stability, including double-strand DNA break (DSB) repair. The central HR protein, RAD51, is frequently overexpressed in human malignancies, thereby elevating HR proficiency and promoting resistance to DNA-damaging therapies. Here, we find that the non-canonical NF-κB factors p100/52, but not RelB, control the expression of RAD51 in various human cancer subtypes. While p100/p52 depletion inhibits HR function in human tumor cells, it does not significantly influence the proficiency of non-homologous end joining, the other key mechanism of DSB repair. Clonogenic survival assays were performed using a pair DLD-1 cell lines that differ only in their expression of the key HR protein BRCA2. Targeted silencing of p100/p52 sensitizes the HR-competent cells to camptothecin, while sensitization is absent in HR-deficient control cells. These results suggest that p100/p52-dependent signaling specifically controls HR activity in cancer cells. Since non-canonical NF-κB signaling is known to be activated after various forms of genomic crisis, compensatory HR upregulation may represent a natural consequence of DNA damage. We propose that p100/p52-dependent signaling represents a promising oncologic target in combination with DNA-damaging treatments.

INTRODUCTION

Homologous recombination (HR) is a highly conserved DNA repair process, which repairs DNA double strand breaks (DSBs) and promotes tolerance of replication-blocking lesions (1,2). In contrast to the error-prone non-homologous end-joining (NHEJ) pathway of DSB rejoining, HR faithfully repairs DNA damage by utilizing an undamaged homologous DNA template to guide the repair process. Since HR facilitates cellular recovery from harmful DNA lesions, cells with deficient HR functionality are highly sensitive to radiation and chemotherapeutic agents that generate DSBs or DNA replication-blocking lesions (3,4). Some components of the HR machinery also serve an important function in stabilizing stalled DNA replication forks (5,6).

The expression of genes that mediate DNA repair is a dynamically regulated process. We previously reported that a family of HR-related genes have variable expression levels, with overexpression occurring in cells that harbor HR defects (7). This overexpression is proposed to act as a compensatory mechanism, particularly since overexpression of the central HR protein RAD51 can partially suppress the HR defects that occur when other key HR genes are downregulated (4,8). We described 20 such DNA repair genes that become overexpressed in this setting, including the key HR-associated genes BRCA1, BRCA2, RAD51, RAD54 and RAD51AP1 (7). Similarly, Bishop and coworkers reported that RAD51, RAD54 and RAD51AP1 become highly transcribed in breast cancers that harbor mutations in the HR-associated gene BRCA1 (8). Taken together, these observations suggest that coordinated transcriptional programs exist to modulate the proficiency of specific repair pathways.

DSB-induced activation of nuclear factor kappaB (NF-κB) is also known to influence cellular resistance to DSB-inducing treatments. Consequently, NF-κB has long been considered a potential therapeutic target for sensitizing tumor cells to DNA-damaging therapies (9). This pro-survival influence of NF-κB activation is partially explained by its classical role in promoting anti-apoptotic responses (10,11). However, its full influence is more complex, given that ATM-dependent activation of NF-κB can influence the proficiency of DNA repair pathways (12–16). For example, early studies demonstrated that knockdown of certain NF-κB subunits was sufficient to reduce expression of FANCD2

*To whom correspondence should be addressed. Tel: +1 773 834 8119; Fax: +1 773 702 0610; Email: philipc.connell@uchospitals.edu

and to sensitize cells to melphalan (16). Subsequent work demonstrated that functional stimulation or inhibition of canonical NF-κB signaling results in corresponding modulation in HR gene expression and DNA repair proficiency (15). Kozono and colleagues exploited this phenomenon using dimethylaminoparthenolide (DMAPT) to radiosensitize cells (14). While DMAPT is a somewhat non-specific inhibitor of NF-κB signaling, it successfully promotes NF-κB-dependent inhibition of both HR and NHEJ. The authors attribute DMAPT's activity to a reduced expression of some repair proteins (FANCD2, BRCA1, RAD51) and reduced chromatin binding by others (Ku80 and XRCC4); however, the functional interactions between NF-κB and DNA repair pathways may be more complex. For example, the key HR protein BRCA1 is known to physically interact with the canonical NF-κB subunit p65 and to augment its ability to activate transcription of NF-κB target genes (17). Furthermore, p65 reportedly interacts directly with the CtIP–BRCA1 complex and promotes processing of DSBs to generate the single-stranded DNA ends that serve as substrates for HR (15). These observations highlight the apparently complex relationships between these pathways.

Most reported connections between NF-κB and DNA repair pathways have focused on canonical NF-κB signaling, wherein target gene transactivation is mediated primarily by the p65 NF-κB subunit (13–16). While canonical NF-κB signaling clearly does affect DNA repair, it also exerts broad influences over other cellular processes ranging from innate/adaptive immune responses to central nervous system development. This presents a central limitation for the strategy of using canonical NF-κB inhibitors to sensitize cancers to DNA-damaging oncology therapies, and it may explain why no direct inhibitors of canonical NF-κB have been approved for clinical use despite decades of drug development efforts (18,19). In this context, some have advocated for therapeutically targeting the non-canonical NF-κB pathway, in which target gene transactivation is primarily mediated by the p52/RelB heterodimer (20,21). Constitutive activation of this pathway has been associated with adverse prognostic features in numerous solid tumor types and hematologic malignancies (21). Additionally, constitutive activation of non-canonical NF-κB upregulates malignant features in experimental tumor models, resulting in faster tumor growth, cellular invasion, and metastasis (22,23).

Given that non-canonical NF-κB is constitutively activated in human malignancies, we sought to characterize its impact on DNA repair and oncologic treatment resistance. Herein we report that the non-canonical NF-κB factor p100/p52 is a key transcriptional regulator of DNA repair proteins, most notably RAD51, the central recombinase that promotes HR. By targeting p100/p52-dependent signaling, we can reduce HR activity in cancer cells and sensitize them to DNA-damaging oncologic treatments in an HR-dependent manner.

MATERIALS AND METHODS

Cell lines

PC-3 cells were a gift from Ralph Weichselbaum. U2OS and 293-HEK cell lines bearing an HR reporter construct (DR-GFP) were gifts from Jeremy Stark and Maria Jasin. Human DLD-1 cell lines are from Horizon Discovery, as is an otherwise identical clone with targeted disruption of BRCA2 at exon 11. PC-3 cells were grown in DMEM:F12 (1:1) with 10% FBS. DLD-1 cells were grown in RPMI-1640 (ATCC formulation) with 10% FBS. All other cell lines were grown in DMEM (high glucose) with 1 mM sodium pyruvate and 10% FBS. Cell lines were tested monthly for mycoplasma contamination using a VenorGem PCR kit (Sigma).

siRNA knockdown and transfection

Cells were treated with siRNAs (or pools thereof) at 75 nM total concentration unless otherwise indicated. siRNAs used include NFKB1 (Ambion AM16704 Assay ID 143856); NFKB2: pool of 5′-CAGCCUAAGCAGAGA GGCU, 5′-CUACGAGGGACCAGCCAAG, 5′-GAUG AAGAUUGAGCGGCCU (Sigma custom siRNAs) or individually and non-silencing control (All Stars Negative Control siRNA, Qiagen 1027281). RNA transfection was carried out using Lipofectamine RNAiMAX (Thermo Fisher 13778150) according to the manufacturer instructions. Cells were incubated with siRNA for 24 h, after which the media was replaced with normal growth media and incubated for a further 24 h to achieve knockdown before conducting experiments unless otherwise indicated.

Cellular proliferation assay

siRNA transfections were performed as above, and 24 h post-transfection cells were re-plated into multiple replicate 96-well plates in fresh medium and allowed to adhere and outgrow. At the end of each time point, one of the replicate plates was developed with CellTiter-Glo reagent (Promega) according to the manufacturer's instructions and luminescence was examined on a Tecan infinite F200 plate reader.

Immunoblots and antibodies

Whole cell extracts were prepared in RIPA buffer (50 mM Tris–HCl pH 8.0, 150 mM NaCl, 1% Igepal CA-630, 0.5% sodium deoxycholate, 0.1% SDS and Roche complete mini protease inhibitors). Sample protein concentrations were determined by BCA assay (Pierce) and the same amount of protein was loaded into each well. Electrophoresed samples were transferred and immobilized onto PVDF membranes and immunoblotted according to antibody manufacturer instructions. The following primary antibodies were used: mouse anti-human NF-κB1 p105/p50 (Santa Cruz 8414), mouse anti-human NF-κB2 p100/p52 (Millipore 05–361), rabbit anti-human RelB (Cell Signaling Technology 4922), rabbit anti-human RAD51 (Pacific Immunology, affinity purified from serum and used at 1:1000), mouse anti-human 53BP1 (Upstate 05-726 Clone BP13), rabbit anti-human H2A.X (Abcam ab229914), mouse anti-human γH2A.X (Millipore 05–636), rabbit anti-human BRCA2 (Bethyl A303-434A), rabbit anti-human GAPDH (Cell Signaling Technology 5174), and mouse anti-chicken α-tubulin (Fitzgerald 10R-T130A). The following secondary antibodies were used: goat anti-rabbit IgG-Alexa Fluor 488 (Life

Technologies A11034), goat anti-mouse IgG-Alexa Fluor 488 (Life Technologies A11001), donkey anti-rabbit IgG-HRP (GE Healthcare NA934V) and sheep anti-mouse IgG-HRP (GE Healthcare NA931V).

RNA-Seq

Total RNA was extracted from three biological replicates of exponentially growing U2OS-DR-GFP cells transfected with non-silencing RNA, siNFKB2 or siRELB using a Qiagen RNeasy Mini kit. All RNA samples were quantified on a Bioanalyzer and had RIN $\geq$ 8.0. Oligo-dT enriched mRNA was run on an Illumina HiSeq 4000 instrument using single end 50 bp reads. For gene-level expression analysis, reads were aligned to the human genome (GRCh38.p13) using STAR 2.7.1a and feature counts were generated using the Subread package 1.6.4; each biological replicate had at least 1.5e7 uniquely-mapped reads. Lowly-expressed genes that did not have at least one count per million in at least two samples were excluded from analysis. Differential expression and pathway analysis were performed using edgeR/limma to determine fold-change in gene expression relative to the non-silencing RNA control; pathways were obtained from the Kyoto Encyclopedia of Genes and Genomes (KEGG) database.

RT-qPCR

Total RNA was extracted from growing cells in buffer containing 10 nM Tris–HCl pH 7.4, 150 nM NaCl, 1% Triton X-100 and 150 mM β-mercaptoethanol, extracted with phenol:chloroform, treated with 3 U DNAse I (New England Biolabs) for 10 min at 37°C, re-extracted with phenol:chloroform, and quantified by UV absorbance. We found that this extraction technique yields RNA of similar yield and quality compared to the kit extraction used for RNA-seq samples above (RIN = 8.5 ± 1.2). For each sample, 250 ng total RNA was annealed to 500 nM oligo-dT, 500 nM random hexamer primers, and incubated with 5 pmol MMLV reverse transcriptase (kindly provided by Dr Song Tan) in 25 μl for 1 h at 42°C. These reactions were diluted in water to provide 0.75 μl equivalent in a 7.5 μl PCR containing 1X Sso Advanced Universal SYBR Green Supermix (Bio-Rad) and 500 nM PCR primers for *RAD51* (5′-TTGGCCCACAACCCATTTCA and 5′-TTAGCTC CTTCTTTGGCGCA), or *COX7C* (5′-TGGTCCGTAGG AGCCACTAT and 5′CGACCACTTGTTTTCCACTGA) and amplified in a CFX384 thermal cycler (Bio-Rad) according to the manufacturer's directions. Primers were designed using NCBI Primer-BLAST. PCRs were performed with two technical replicates per sample along with corresponding no-reverse transcriptase and no-template controls. Cq values were calculated automatically in Bio-Rad CFX Manager software (version 3.1).

Immunocytochemistry

Cells were seeded onto glass coverslips 24 h after addition of siRNA/lipid complexes and allowed to grow for another 24 h prior to a 1-h pulse with 10 μM 5-ethynyl-2′-deoxyuridine (EdU, Lumiprobe) ± 30 nM camptothecin (CPT, Alfa Aesar), followed by the indicated outgrowth time in fresh medium. Samples were fixed in 3.0% PFA in PBS with 3.4% sucrose, and permeabilized with 0.5% Triton X-100 in 20 mM HEPES pH 7.4, 50 mM NaCl, 3 mM $MgCl_2$ and 300 mM sucrose. EdU was fluorescently labeled using click chemistry: samples were incubated in freshly-prepared 1× TBS with 2 mM $CuSO_4$, 20 mM sodium ascorbate, 10% DMSO and 5 μM sulfo-cyanine-5-azide for 30 min at room temperature. Immunostaining was performed by blocking in 1% BSA in PBS for 20 min at room temperature, staining with primary antibody at 1:1000 for 2 h at room temperature, followed by fluorescent secondary antibody at 1:1000 for 1 h at room temperature. Coverslips were mounted with Vectashield with DAPI (Vector Laboratories, H-1200) and imaged on a Zeiss M.1 Axiovision fluorescent microscope at 1000× total magnification. For data sets of unselected nuclei, at least 213 nuclei per condition were imaged and for all samples at least 100 EdU-positive nuclei were imaged. Image analysis was carried out using CellProfiler.

DSB repair reporter assays

U2OS and 293-HEK cells bearing reporter constructs were transfected with siRNAs. After 24 h, siRNA transfectants were collected by trypsinization and electroporated with 30 μg pCAGGS or pBASce in 0.8 ml Opti-MEM (Gibco) in 4 mm cuvettes at 325 V, 975 μF, 15–20 ms pulse time, seeded into six-well plates with complete media, and grown for an additional 48 h. Transfectants were collected by trypsinization, resuspended in PBS containing 1 μg/ml 7-aminoactinomycin D (7-AAD), and analyzed on a BD LSR-II cytometer. Live non-apoptotic cells were selected on a forward scatter versus side scatter plot followed by gating out 7-AAD positive cells, and GFP positive cells were selected on an orange versus green plot.

Cell cycle analysis

Growing cells were collected by trypsinization, fixed with 4% paraformaldehyde in PBS, permeabilized with 0.5% Triton X-100 in PBS, and stained with 10 μg/ml DAPI in PBS with 1% BSA, 0.5% Triton X-100, and 1 mM EDTA. Single cells were analyzed on a BD Fortessa X-20 cytometer for DAPI content. G1, S and G2 cell populations were determined by univariate modelling in FlowJo software.

Clonogenic survival

Cells were plated at an appropriate density (800–2000 cells per well) into six-well plates in complete medium with the indicated dose of camptothecin and grown until colonies of >50 cells appeared in the control wells. For IR treatment, cells were re-plated as above 24 h after siRNA transfection and allowed to attach for an additional 24 h, after which X-rays were administered using a Philips Maxitron RT250 irradiator. Colonies were fixed and stained with 6% glutaraldehyde, 0.5% crystal violet, photographed and enumerated using an in-house developed macro for ImageJ.

Statistical analysis

Data for protein expression quantitation, average RAD51 foci per nucleus, percent GFP + cells, cell cycle distribution and clonogenic survival are presented as the mean ± SEM. Differences between the means of two groups were analyzed by unpaired two-tailed Student's *t*-test. Differences in cell cycle distributions between two groups were analyzed using Hotelling's *T*-squared distribution. Differences in EdU-positive cells between two conditions were analyzed by Pearson's chi-squared test. Differences in cytological foci per nucleus and colony size between two conditions was determined by Wilcoxon Rank-Sum test. *P*-values <0.05 were considered to be significant for these tests. For RNA-seq data, differences in individual gene expression levels between two conditions were examined by two-tailed exact test for the negative binomial distribution, with p-values adjusted for multiple testing by the Benjamini and Hochberg method (24). Publicly-available microarray data for mice overexpressing p52 and wild-type littermate controls (GEO GSE71648) were RMA-normalized using the 'oligo' package for Bioconductor, filtered to remove probes that map to multiple genes, fitted to a linear model using the 'limma' package, and differential expression was determined by applying an empirical Bayes method to the fitted data. Each of the two groups of mice contained two biological replicates (25). Differences in KEGG pathway enrichment analysis between two conditions were tested by one-tailed Fisher's exact test. For RT-qPCR, relative gene expression was determined by the ddCq method using *COX7C* as the reference gene (dCq = Cq[*RAD51*] – Cq[*COX7C*]) and the non-silencing control samples as reference samples (ddCq = dCq[siNFKB2] – dCq[siNS]); *COX7C* was selected as the reference gene based on its relatively high and invariant expression observed in the RNA-seq data. All statistical testing and graphing were performed in R.

RESULTS

Disruption of p100/p52 in human tumor cells reduces the expression of RAD51 and other HR-promoting genes

Prior studies have demonstrated that canonical NF-κB signaling controls the expression of DNA repair proteins and the functional proficiency of these pathways (13–16). We questioned whether p100/p52 and/or RelB, which are central mediators of non-canonical NF-κB signaling, also exert influences on DNA repair. If so, we hypothesized that targeting of this pathway may offer a relatively tolerable oncologic treatment approach.

RNA-seq was performed 48 h after treatment with siRNAs that target *NFKB2* or *RELB* in human osteosarcoma (U2OS) cells. Efficient knockdown was achieved for both p100/p52 and RelB at the mRNA and protein levels (Figure 1A, Supplementary Figure S1a). In addition to reducing p100/p52 levels, siNFKB2 also reduces RelB expression; this is expected since p100/p52 is known to bind and stabilize RelB protein (26). To predict the impact on biological processes, global gene expression changes were analyzed using over/under-representation of Kyoto Encyclopedia of Genes and Genomes (KEGG) terms to predict the 10 most upregulated and 10 most downregulated pathways (Figure 1B). Using a threshold of $P < 0.01$, this identified HR as the only DSB repair pathway significantly affected by siNFKB2 ($P < 10^{-4}$). By comparison, these data suggest that siRELB is not predicted to influence HR (Supplementary Figure S1b). *NFKB2* knockdown in U2OS cells also has predicted effects on additional genomic housekeeping functions, including DNA replication, mismatch repair, base excision repair, and the Fanconi Anemia pathway.

Given this regulation of HR by p100/p52, we focused on transcriptional regulation of 39 select genes with known relevance to HR, as defined by the KEGG database (release 91). In response to siNFKB2, only two HR-related genes are significantly ($P < 0.01$) upregulated (Figure 1C, Supplementary Figure S1c, d). 14 HR-related genes are significantly ($P < 0.01$) downregulated. Of these 14 genes, *RAD51* is the most differentially expressed gene (4.5-fold downregulated, $P < 10^{-42}$).

NFKB1 or *NFKB2,* which encode p105/p50 and p100/p52 proteins, respectively, were transcriptionally targeted using siRNA. Parallel experiments were performed using three human cells lines derived from a wide range of malignancies, including prostate carcinoma (PC-3), osteosarcoma (U2OS), and colorectal carcinoma (DLD-1). Consistent with prior reports (14), we find that p105/p50 controls the expression of RAD51 protein, the central recombinase that mediates HR. Additionally, we find that p100/p52 similarly controls RAD51 protein at the transcriptional level (Figure 2A, B, Supplementary Figure S2a–d). This significant effect by siNFKB2 persists up to 4 days following siRNA transfection and is reproducibly confirmed using various individual siRNAs to silence expression (Figure 2C, Supplementary Figure S2e). While KEGG pathway analyses had suggested that DNA replication and cell cycle pathways are downregulated upon *NFKB2* disruption (Figure 1B), this effect appears to be modest since we observe only a slight reduction in cellular proliferation for U2OS cells and no effect on proliferation for PC-3 and DLD-1 cells transfected with siNFKB2 (Supplementary Figure S2f). By comparison, knockdown of the canonical NF-κB pathway with siNFKB1 induces significant growth abnormalities in all three cell lines.

Finally, we asked whether forced overexpression of p52 might induce an increase in *RAD51* expression. This was accomplished by examining publicly-available data from Saxon and colleagues, who performed forced overexpression of FLAG-tagged p52 in mouse lung tissue (27). Indeed, we find that p52 overexpression induces a significant increase in the transcription of *Rad51* (Figure 2D).

Disruption of p100/p52 in human tumor cells inhibits damage-induced RAD51 focus formation in S-phase cells

The initial steps of HR involve 5′ to 3′ nuclease activity that generates a 3′ single-stranded DNA (ssDNA) tail at the site of damaged DNA (2). This ssDNA tail becomes coated with Replication Protein A (RPA), which is subsequently replaced by a helical filament of RAD51 protein. The displacement of RPA by RAD51 is facilitated by several mediator proteins, which include BRCA2 and RAD51 paralog complexes. Since RAD51 filaments can be imaged as sub-

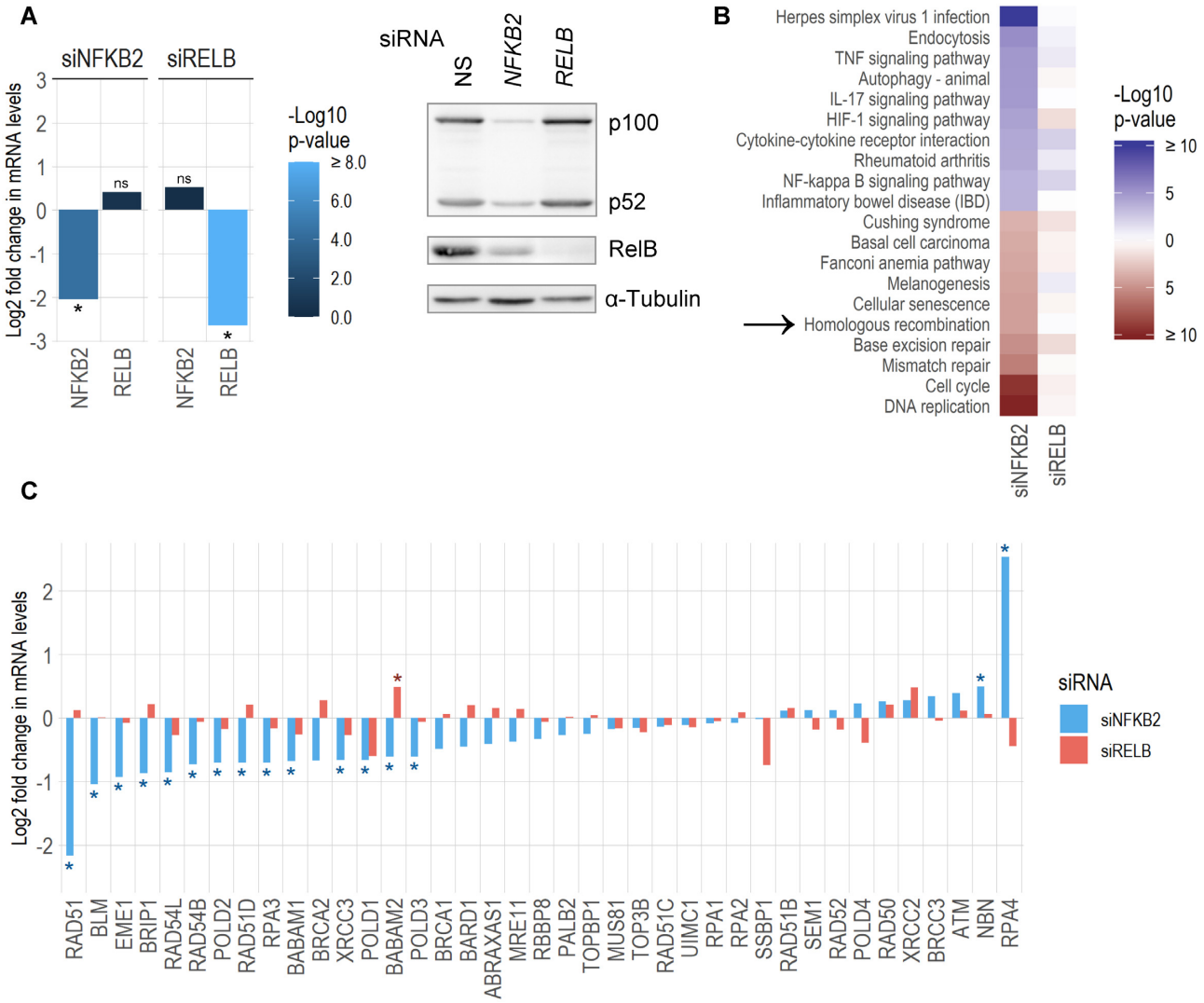

Figure 1. Targeting of p100/p52 promotes a transcriptional downregulation of RAD51 and other proteins known to control DSB repair by HR. RNA-seq was performed on U2OS cells transfected with non-silencing (NS), *NFKB2* or *RELB* siRNA. (**A**) Knockdown is efficient for both p100/52 and RelB, based on mRNA measurements by RNA-seq (left) and protein level by western blot (right). (**B**) KEGG pathway analysis of was performed to predict the 10 most upregulated and 10 most downregulated pathways in response to siNFKB2. Corresponding effects in response to siRELB are also displayed. (**C**) Expression levels are displayed for 39 genes with known relevance to HR, as defined by the KEGG database. Genes are arrayed from left to right based on degree of expression change after siNFKB2 (* denotes $P < 0.01$).

nuclear foci, immunofluorescence microscopy is commonly utilized to directly visualize HR intermediates in cells (28).

The impact of siNFKB2 on RAD51 focus formation was tested, again using PC3, U2OS, and DLD-1 cancer cell lines. To focus on dynamic changes occurring during replication, we simultaneously pulsed cells with 5-ethynyl-2′-deoxyuridine (EdU) to mark S-phase cells, and treated cells with camptothecin (CPT) to induce replication-associated DSBs (Figure 3A, B). As predicted, the targeting of p100/p52 reduces the appearance of CPT-induced RAD51 foci in replicating (i.e. EdU+) cells. The impact of siNFKB2 on HR proficiency cannot be explained by non-specific effects on S-phase dynamics, since siNFKB2 does not influence EdU incorporation in PC-3 or DLD-1 cells (Figure 3C). Of note, siNFKB2 does modestly reduce EdU incorporation in U2OS cells (46% versus 37%, $P = 0.049$); this finding is consistent with our KEGG pathway analysis, which had predicted that modest replication alterations may occur in this specific condition (Figure 1B). The inhibitory effect of siNFKB2 on HR persists for at least 7 h after CPT treatment, indicating that HR suppression persists throughout S/G2 (Figure 3D, E). Even at 24 h after CPT treatment, a significant number of unrepaired DSBs persist in the siNFKB2 treated cells (Supplemental Figure S3).

Disruption of p100/p52 in human tumor cells inhibits HR proficiency

We tested whether disruption of p100/p52 influences HR proficiency using functional reporters in cancer cells. The DR-GFP assay relies on a stably-integrated reporter construct that carries two non-functional copies of green fluo-

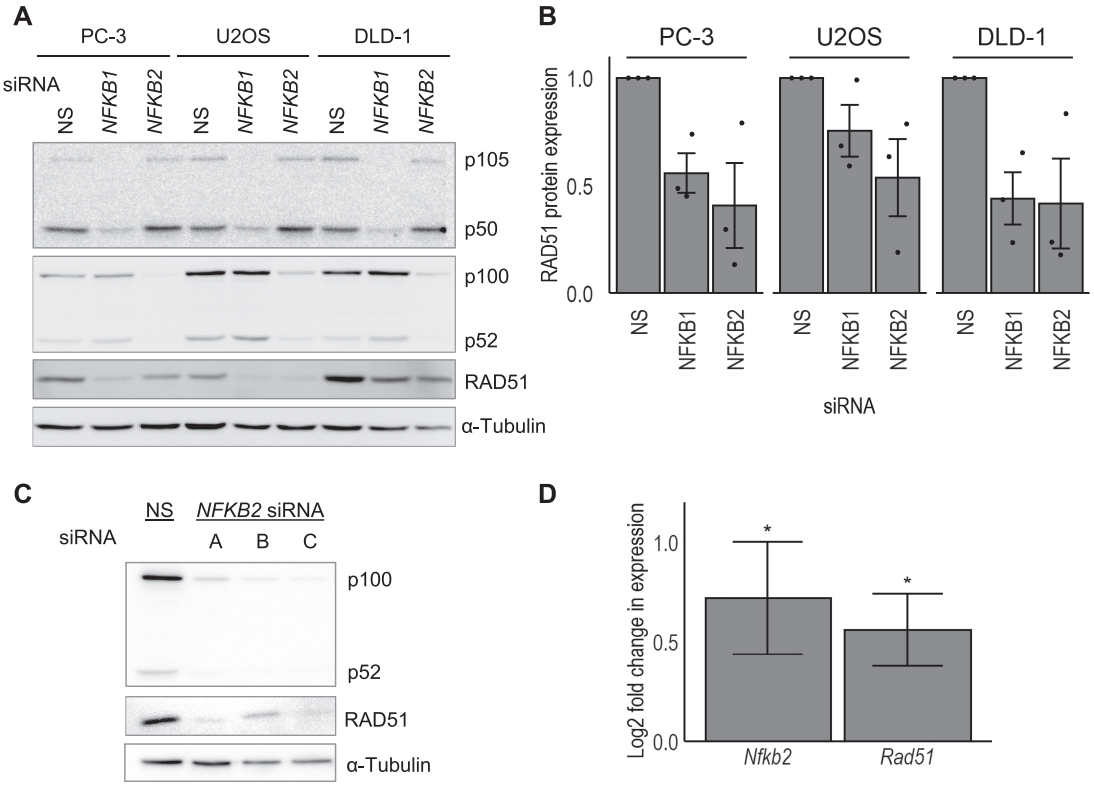

Figure 2. Targeting of p100/p52 promotes downregulation of RAD51 protein. (**A**) Representative western blots demonstrate that transcriptional silencing of key NF-κB proteins leads to reduced levels of RAD51 protein. (**B**) Quantitation of western blots from three independent experiments demonstrate that RAD51 reductions after siNFKB2 are reproducible (error bars denote the SEM). (**C**) Comparable levels of RAD51 knockdown are observed using three different siRNAs (each at 25 nM) targeting *NFKB2* in U2OS cells. (**D**) Forced overexpression of the p52 fragment of *Nfkb2* in mouse lung tissue is associated with increased *Rad51* expression (error bars denote standard error, * denotes $P < 0.02$, NS denotes non-silencing control).

rescence protein (GFP), one of which is interrupted by an I-SceI endonuclease site (29). Induction of a DSB at the I-SceI site prompts repair by HR-mediated gene conversion that generates a functional copy of GFP.

The impact of siNFKB2 on HR proficiency was tested using two separate human cell lines, both stably transfected with a single copy of the DR-GFP cassette. Indeed, the targeting of p52-dependent signaling reduces HR proficiency by 71.7% in U2OS cells ($P = 0.009$, 95% CI 52.2% to 91.3%), and by 50.2% in HEK-293 cells ($P = 1.1e{-}9$, 95% CI 46.3% to 54.1%) (Figure 4A, B). Mirroring our finding regarding S-phase dynamics, the impact of siNFKB2 on HR proficiency cannot be explained by non-specific effects on S-phase entry, since siNFKB2 does not significantly influence the portion of cells in S-phase in HEK-293 cells carrying the DR-GFP cassette (Figure 4C, Supplementary Figure S4a). We find that siNFKB2 does exert a small effect on cell cycle in U2OS cells; this again suggests that p100/p52 loss exerts a modest impact on DNA replication in at least some cell types, which is consistent with our prior functional predictions in U2OS cells (Figure 1B).

We next asked whether disruption of p100/p52 influences efficiency of single-strand annealing (SSA). The SSA is a pathway that repairs DSBs occurring between a pair of tandem-repeated sequences, such that single-strand degradation from the site of the DSB creates a pair of ssDNA tracts with an extensive complementary sequence (30). The two ssDNA tails then anneal to heal the DSB, and the DNA originally located between the repeats is thereby deleted. SSA does not involve the NHEJ pathway, nor does it require most HR-related proteins (31). Interestingly, SSA efficiency is known to be elevated in situations where RAD51 function has been disrupted by a variety of means (32–35). As expected, we find that disruption of p100/p52 does increase SSA by a modest 14.5% ($P = 0.032$, 95% CI 4.5% to 24.4%) (Figure 4D, Supplementary Figure S4b).

Disruption of p100/p52 in human tumor cells preserves the function of NHEJ

We next investigated whether the disruption of p100/p52 affects NHEJ, the other major mechanism for DSB repair. This is an important consideration, since prior NF-κB targeting methodologies have demonstrated relatively non-specific effects on various DNA repair processes. For example, treatment with DMAPT inhibits the proficiency of both HR and NHEJ (14). Likewise, experimental changes in p65 activity modulate the proficiency of both HR and NHEJ (15).

Therefore, we tested the impact of siNFKB2 on HEK-293 cells, which carry a single copy of a stably-integrated GFP-based reporter of NHEJ (32). Disruption of p100/p52 does not significantly impact NHEJ function in asynchronous cells (Figure 5A, B). We additionally asked

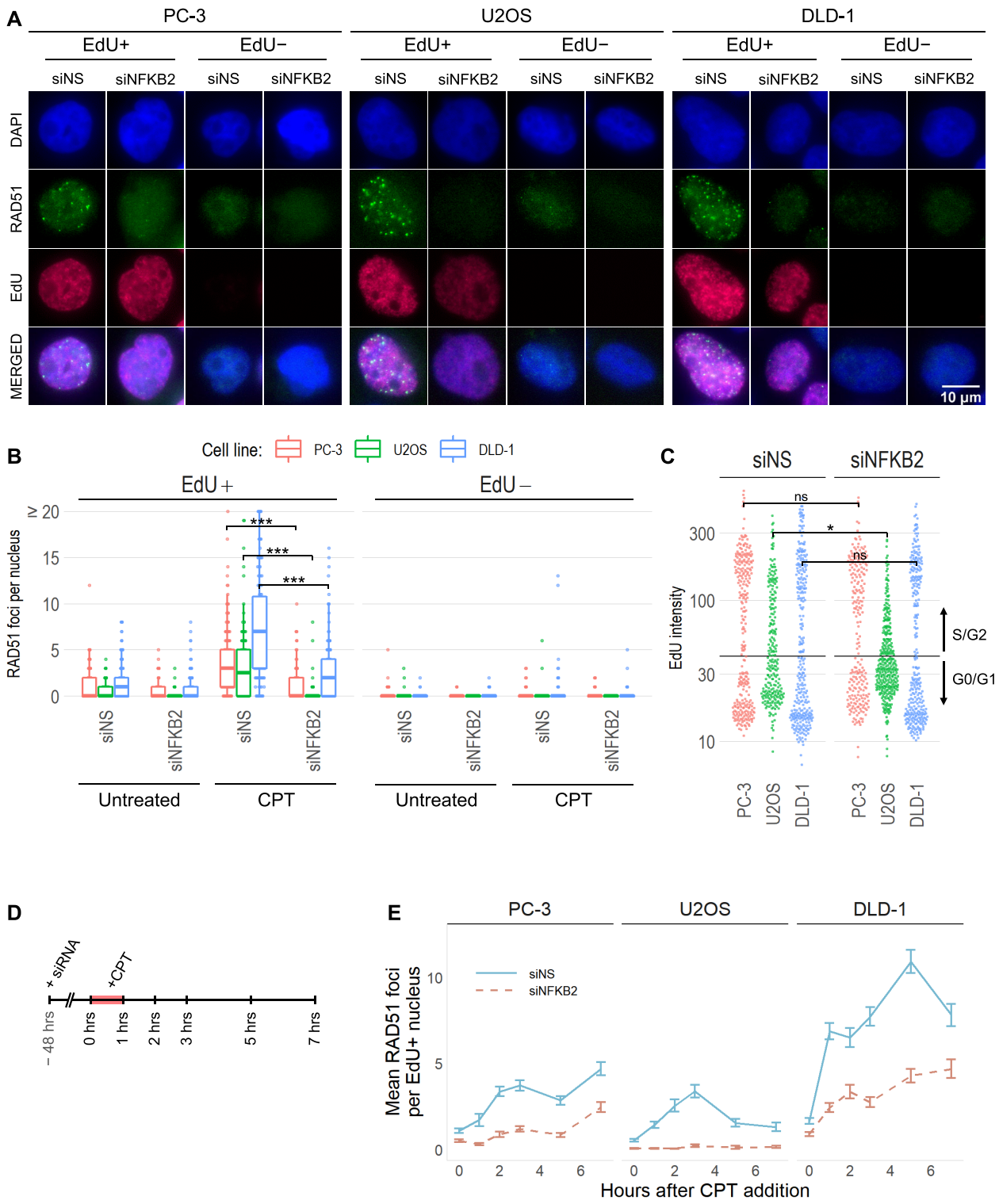

Figure 3. Targeting of p100/p52 inhibits DNA damage-induced RAD51 focus formation in human cancer cells. Cells previously transfected with siRNA or non-silencing (NS) controls were pulse-labeled with EdU to mark S-phase cells and concomitantly treated with 30 nM CPT for 1 hour. Cells were harvested and immune-stained as indicated. Representative microscopic images of unselected nuclei (**A**) are displayed for cells collected 3-hours after CPT treatment, and (**B**) quantitation of RAD51 foci per nucleus is plotted for each of the indicated conditions. (**C**) Quantitation of EdU intensity in CPT-untreated cells is used to estimate cell cycle at the time of the EdU pulse. (**D**) A schematic representation of the treatment timeline is displayed. (**E**) The mean number of RAD51 foci per EdU-positive nucleus is plotted as a function of time following CPT treatment (error bars denote SEM for at least 100 nuclei within a single experimental replicate, * denotes $P < 0.05$, *** denotes $P < 1e{-}13$, and ns denotes $P > 0.05$).

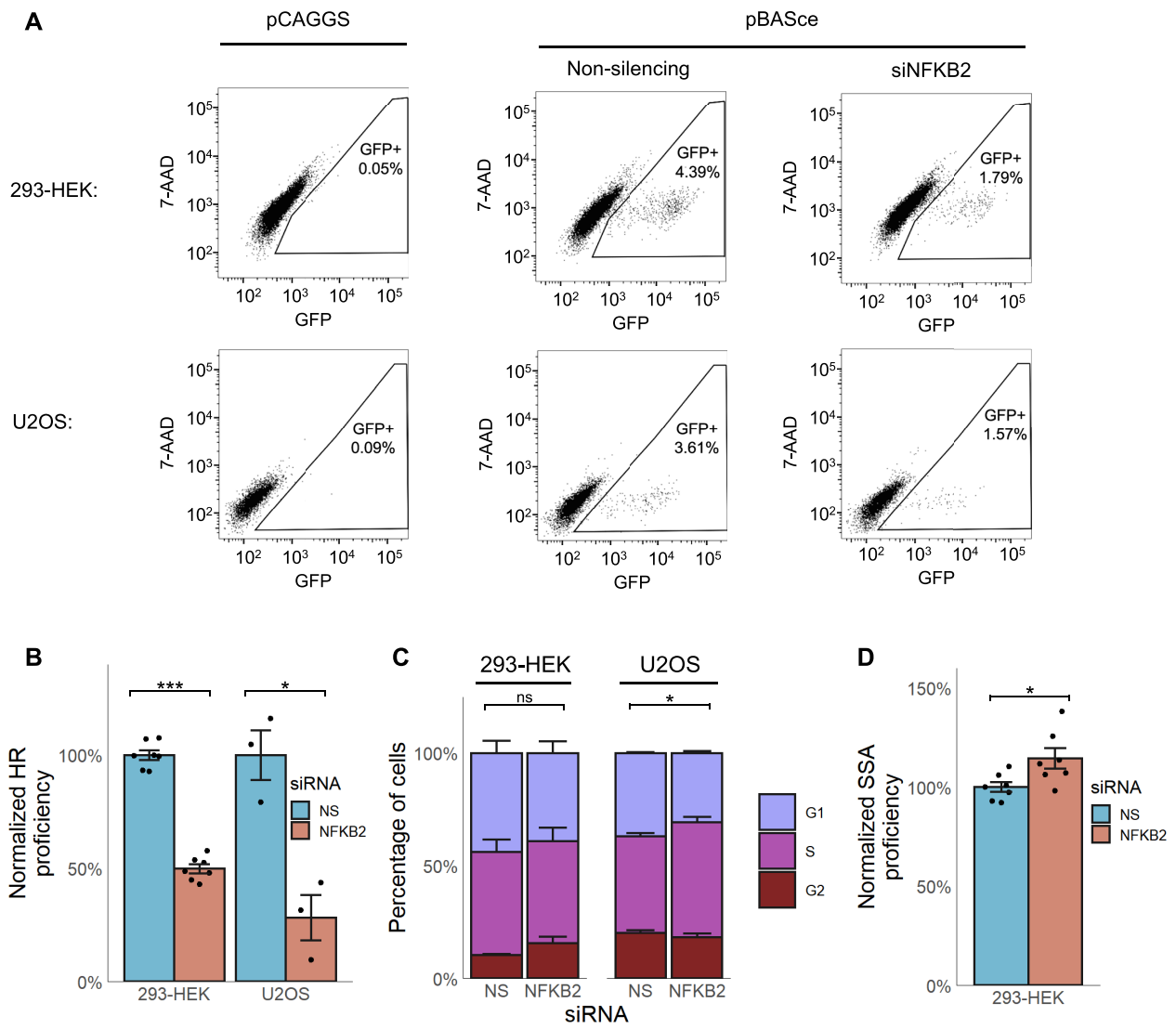

Figure 4. Targeting of p100/p52 inhibits HR function. Two human cancer cell lines with integrated HR reporter constructs (DR-GFP) were treated with siNFKB2 or a non-silencing control (NS). (**A**) Cells were transfected with a plasmid (pBASce) that directs expression of I-SceI nuclease or an empty vector (pCAGGS). Representative scatter plots of flow cytometry data demonstrate that siNFKB2 reduces HR-mediated gene conversion and resulting GFP expression. (**B**) Effects on HR proficiency are plotted for at least three experimental replicates. (**C**) Flow cytometry was performed to measure DNA content in treated cells. Effects on cell cycle distribution are plotted for three experimental replicates. (**D**) Effects on SSA proficiency are plotted for seven experimental replicates. Error bars denote SEM, * denotes $P < 0.05$, and *** denotes $P < 1e{-}8$.

whether p100/p52 loss affects the appearance NHEJ intermediates in replicating cells. This was tested using a similar methodology to that used for quantifying HR intermediates following DSB induction with CPT (Figure 5C). We find that siNFKB2 does not prevent the appearance of damage-induced p53-binding protein 1 (53BP1) foci or their timely resolution in replicating cells (Figure 5D, E). Taken together, these results indicate that the targeting of p100/p52 specifically reduces HR-mediated DSB repair.

Targeting of p100/p52-dependent signaling leads to HR-dependent sensitization to CPT treatment

We next examined whether targeting of p52-dependent signaling represents a potential therapeutic strategy in oncology. We chose to focus on CPT-induced DNA damage, since topoisomerase I (Top1) inhibitors are selectively toxic to S-phase cells (36). CPT leads to accumulation of Top1 cleavage complexes on DNA, and single-stranded DNA breaks are converted to DSBs when replication forks collide with these complexes (37). Importantly, cells are particularly reliant on HR for repairing CPT-induced DSBs (38).

Clonogenic survival assays were performed using an isogenic pair of colorectal adenocarcinoma cell lines that differ only in their expression of a key HR protein, BRCA2. As predicted, the disruption of p100/p52 leads to CPT sensitization in BRCA2-competent cells (Figure 6A). By contrast, CPT sensitization is absent in cells that lack BRCA2. This sensitization in HR-competent cells is not caused by differences in cellular proliferation, since p100/p52 loss does

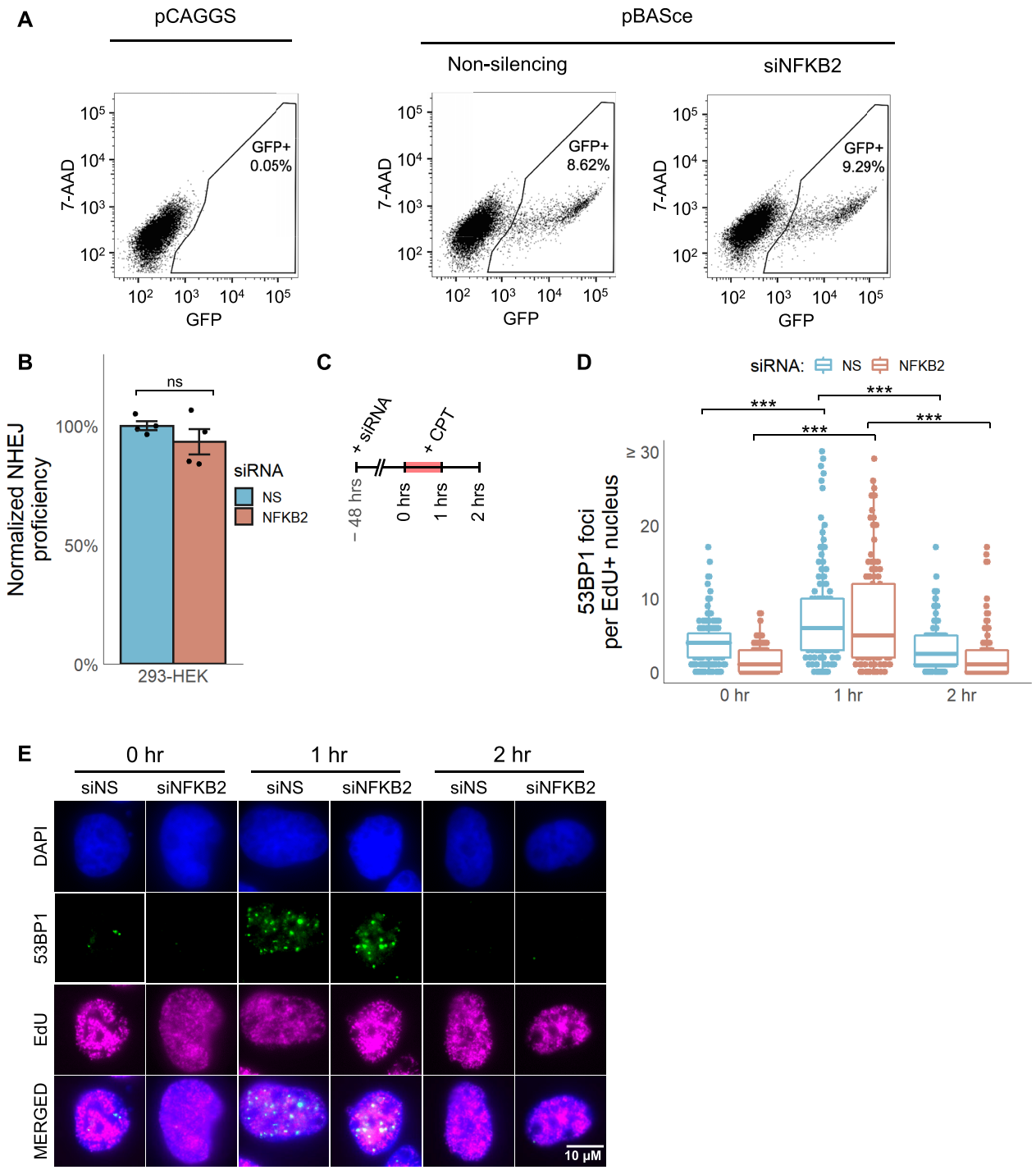

Figure 5. Targeting of p100/p52 does not significantly affect DSB repair by non-homologous end joining. (**A**) 293-HEK cell lines carrying an integrated NHEJ reporter construct (EJ5-GFP) were treated with siNFKB2 or a non-silencing (NS) control. Cells were transfected with a plasmid (pBASce) that directs expression of I-SceI nuclease or an empty vector (pCAGGS). Representative scatter plots of flow cytometry data demonstrate that siNFKB2 does not significantly reduce DSB repair by NHEJ. (**B**) These effects on NHEJ are plotted for four experimental replicates, and error bars denote SEM (ns denotes $P > 0.05$). (**C**) A schematic representation of the treatment timeline is displayed for time course experiment using U2OS cells. (**D**) 53BP1 foci per nucleus are quantified (*** denotes $P < 1e{-}5$), and (**E**) representative nuclei images are shown for each treatment.

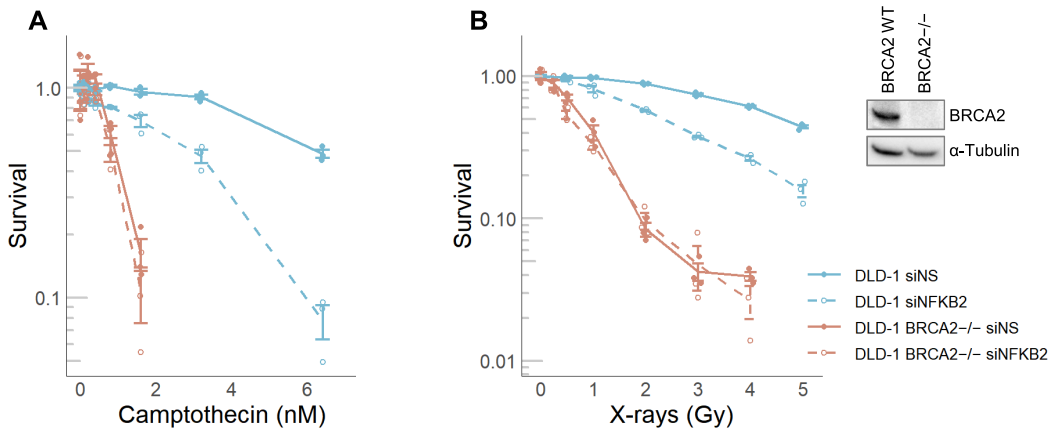

Figure 6. Targeting of p100/p52 specifically sensitizes HR-proficient cells to DNA-damaging treatments. Clonogenic survival is plotted for DLD-1 cells and an isogenic BRCA2−/− derivative incubated continuously with (**A**) indicated doses of camptothecin or treated with a (**B**) single dose of ionizing radiation. Error bars represent SEM for three replicates.

not significantly alter the growth rate of these DLD-1 based cell lines (Supplementary Figure S2f, 5B). The sensitization is also not caused by variable levels of CPT-induced DNA breaks, since comparable levels of γH2A.X phosphorylation are induced by CPT regardless of p100/p52 status (Supplementary Figure S5c). Finally, this sensitization is not related to unintended changes in RelB levels (as was observed in Figure 1A), since siRelB does not sensitize DLD-1 cells to CPT (Supplementary Figure S5d).

We repeated these experiments using ionizing radiation in place of CPT. Again, the disruption of p100/p52 leads to significant sensitization in BRCA2-competent cells, while radiation sensitization is absent in DLD-1 derivatives that lack BRCA2 (Figure 6B). Taken together, these results demonstrate that p100/p52 promotes resistance to DSB-causing treatments by supporting HR-mediated DSB repair.

DISCUSSION

Herein, we demonstrate that the non-canonical NF-κB factor p100/p52 is a key transcriptional regulator of DNA repair proteins, most notably RAD51, the central recombinase that promotes HR. Inhibition of p100/p52-dependent signaling leads to a robust reduction in HR activity in cancer cells, thereby sensitizing them to DNA-damaging oncologic treatment in a manner that is specific to HR. While various other HR-related genes are also downregulated after p100/p52 targeting, *RAD51* is the most differentially expressed gene and is likely a central driver of this response.

We propose that p100/p52-dependent signaling promotes compensatory HR in response to genomic insults. This builds on recent studies demonstrating that non-canonical NF-κB signaling is activated after various forms of genomic crisis. For example, both radiation-induced DSBs and genomic instability can promote the liberation of nucleic acids into the cytoplasm after mitosis, which ultimately leads to the activation of non-canonical NF-κB (22,39). In this context, we propose that HR upregulation represents a natural consequence of DNA damage. This concept is supported by our prior work demonstrating that *RAD51* is overexpressed in cells that harbor DNA repair defects or stigmata of genomic instability (e.g. DNA copy number variations, estrogen receptor loss, and *HER2* amplification) (7,40). Other groups have similarly observed overexpression of HR proteins in cells harboring repair-deficient states (41,42). Compensatory upregulation of RAD51 protein levels may be especially impactful in this context because RAD51 overexpression can functionally compensate for other causes of HR deficiency (4,8). Expression changes in other DNA repair proteins may also contribute to the functional HR upregulation. For example, RAD54 and RAD51AP1 are known to be overexpressed in *BRCA1*-mutant breast tumors (8), and MRE11 is overexpressed in radiation-sensitive bladder tumors (43). Both may represent clinical examples wherein compensatory HR upregulation occurs in response to chronic endogenous DSB repair deficiencies.

Additional DNA repair pathways have been reported to have altered regulation in response to HR loss and genomic instability. For example, DNA polymerase θ (Polθ) is overexpressed in BRCA1-deficient cell lines, and this overexpression can be reversed by BRCA1 complementation (43). Since Polθ promotes MMEJ, this implies that mutation-prone DNA repair mechanisms become upregulated in cancers as a means to compensate for HR loss (44,45). We observed no significant changes in Polθ expression in response to p100/p52 loss (Supplementary Figure S1d). We did, however, find that targeting of p100/p52 increases the functional proficiency of error-prone SSA (Figure 4D). We also observed expression changes that predict that other genome maintenance pathways (DNA replication, base excision repair, and mismatch repair) may be functionally modulated (Figure 1B). Interestingly, we also observed a significant, 5.8-fold, upregulation in Replication Protein A 30 kDa subunit (RPA4) in response to p100/p52 depletion (Figure 1C). The RPA heterotrimeric protein complex is responsible for binding and stabilizing ssDNA in eukaryotic cells, and in general this complex is composed of the subunits RPA1 (70kDa subunit), RPA2 (32kDa subunit) and RPA3 (14kDa subunit) (46,47). Under certain circumstances that remain

incompletely understood, RPA4 can replace RPA2 in the heterotrimer complex, thereby yielding an alternative RPA (aRPA) complex (48). Although the aRPA complex does not support DNA replication, it may support the early steps of nucleotide excision repair or HR (49,50). Further work is needed to better understand the significance of RPA4 up-regulation after p100/p52 depletion.

The genome-wide landscape of promoter/enhancer elements bound by NF-κB subunits has been characterized previously (51). These and other published results suggest that *RAD51*′s promoter/enhancer elements might not be directly bound by NF-κB subunits (52). It's possible, for example, that p100/p52-dependent regulation of *RAD51* occurs through an indirect mechanism. E2F transcription factors (TFs) are known to bind *RAD51*′s promoter (52,53), and E2F TFs are transcriptionally regulated by NF-κB subunits (51,54). Taken together, p52 may regulate *RAD51* transcription indirectly by modulating E2F TFs. Further work is underway to test this and other competing possibilities. For example, target gene transactivation can be influenced by p52 homodimers and by p52-p65 heterodimers (55). Additionally, phosphorylated Bcl3 can form a ternary complex with p52 to regulate transcriptional activity (56–58). Finally, ETS-1 and p52 were recently shown to directly interact, forming a heterotetrametric complex that can bind promoter elements and influence gene expression (59). In some settings, the ETS-1–p52 complex acts as a transcriptional activator, while free ETS-1 acts as a transcriptional repressor. A potential role for ETS-1 in mediating our observed HR effects is intriguing, since ETS-1 has been implicated in the regulation of some HR genes (60,61), and since *RAD51*′s protomer contains an ETS-1 binding motif (52). Other, more remote mechanistic explanations might also be considered. For example, cytoplasmic p100 is known to bind and sequester p65, thereby reducing its activity by preventing its nuclear localization (62,63), and therefore depletion of p100 might conceivably affect HR indirectly by modulating canonical NF-κB signaling. Our ongoing work will clarify these remaining open questions.

This work has practical relevance to evolving pharmacologic strategies for inhibiting non-canonical NF-κB signaling (21). This pathway may represent a relatively tolerable therapeutic target in oncology, since pharmacologic inhibition of its functions in normal tissues (e.g. lymphoid organ development, B cell survival and maturation, and differentiation of osteoclasts) are predicted to be relatively tolerable (55,64,65). Small molecules have been developed to selectively bind the inhibitory kappa B kinase α (IKKα), an upstream kinase that governs pathway activation (20). A competing approach targets NF-κB-inducing kinase (NIK), which governs the non-canonical NF-κB cascade by phosphorylating IKKα (66,67). It is worth noting, however, that the NIK-IKK signaling axis acts as a master regulator of additional processes, and therefore these inhibitory compounds may exert wide-ranging effects that are off-target relative to non-canonical NF-κB signaling (20).

In summary, we find that p100/p52 dependent signaling controls the proficiency of HR in human cells. Since non-canonical NF-κB is constitutively upregulated in human tumors, drug discovery programs aimed at overcoming p100/p52-dependent signaling may offer a means to overcome therapeutic resistance and improve oncology patient outcomes.

DATA AVAILABILITY

RNA-seq data have been deposited on the GEO (GSE148511).

SUPPLEMENTARY DATA

Supplementary Data are available at NAR Online.

ACKNOWLEDGEMENTS

We thank Douglas Bishop, Ralph Weichselbaum and Bakhtiar Yamini for helpful conversations, reagents, and/or for critical reviews of the manuscript.

FUNDING

National Institutes of Health [2R01CA142642 to P.P.C.] Funding for open access charge: National Institutes of Health.
Conflict of interest statement. None declared.

REFERENCES

1. Tebbs,R.S., Zhao,Y., Tucker,J.D., Scheerer,J.B., Siciliano,M.J., Hwang,M., Liu,N., Legerski,R.J. and Thompson,L.H. (1995) Correction of chromosomal instability and sensitivity to diverse mutagens by a cloned cDNA of the XRCC3 DNA repair gene. *Proc. Natl. Acad. Sci. U.S.A.*, **92**, 6354–6358.
2. Thompson,L.H. and Schild,D. (2001) Homologous recombinational repair of DNA ensures mammalian chromosome stability. *Mutat. Res.*, **477**, 131–153.
3. Liu,N., Lamerdin,J.E., Tebbs,R.S., Schild,D., Tucker,J.D., Shen,M.R., Brookman,K.W., Siciliano,M.J., Walter,C.A., Fan,W. *et al.* (1998) XRCC2 and XRCC3, new human Rad51-family members, promote chromosome stability and protect against DNA cross-links and other damages. *Mol. Cell*, **1**, 783–793.
4. Takata,M., Sasaki,M.S., Tachiiri,S., Fukushima,T., Sonoda,E., Schild,D., Thompson,L.H. and Takeda,S. (2001) Chromosome instability and defective recombinational repair in knockout mutants of the five rad51 paralogs. *Mol. Cell. Biol.*, **21**, 2858–2866.
5. Schlacher,K., Christ,N., Siaud,N., Egashira,A., Wu,H. and Jasin,M. (2011) Double-strand break repair-independent role for BRCA2 in blocking stalled replication fork degradation by MRE11. *Cell*, **145**, 529–542.
6. Ying,S., Hamdy,F.C. and Helleday,T. (2012) Mre11-dependent degradation of stalled DNA replication forks is prevented by BRCA2 and PARP1. *Cancer Res.*, **72**, 2814–2821.
7. Pitroda,S.P., Pashtan,I.M., Logan,H.L., Budke,B., Darga,T.E., Weichselbaum,R.R. and Connell,P.P. (2014) DNA repair pathway gene expression score correlates with repair proficiency and tumor sensitivity to chemotherapy. *Sci. Transl. Med.*, **6**, 229ra242.
8. Martin,R.W., Orelli,B.J., Yamazoe,M., Minn,A.J., Takeda,S. and Bishop,D.K. (2007) RAD51 up-regulation bypasses BRCA1 function and is a common feature of BRCA1-deficient breast tumors. *Cancer Res.*, **67**, 9658–9665.
9. Jung,M. and Dritschilo,A. (2001) NF-kappa b signaling pathway as a target for human tumor radiosensitization. *Semin. Radiat. Oncol.*, **11**, 346–351.
10. Wang,C.Y., Cusack,J.C. Jr, Liu,R. and Baldwin,A.S. Jr (1999) Control of inducible chemoresistance: enhanced anti-tumor therapy through increased apoptosis by inhibition of NF-kappaB. *Nat. Med.*, **5**, 412–417.
11. Wang,C.Y., Mayo,M.W. and Baldwin,A.S. Jr (1996) TNF- and cancer therapy-induced apoptosis: potentiation by inhibition of NF-kappaB. *Science*, **274**, 784–787.

12. Aasland,D., Gotzinger,L., Hauck,L., Berte,N., Meyer,J., Effenberger,M., Schneider,S., Reuber,E.E., Roos,W.P., Tomicic,M.T. *et al.* (2019) Temozolomide induces senescence and repression of DNA repair pathways in glioblastoma cells via activation of ATR-CHK1, p21, and NF-kappaB. *Cancer Res.*, **79**, 99–113.
13. Cron,K.R., Zhu,K., Kushwaha,D.S., Hsieh,G., Merzon,D., Rameseder,J., Chen,C.C., D'Andrea,A.D. and Kozono,D. (2013) Proteasome inhibitors block DNA repair and radiosensitize non-small cell lung cancer. *PLoS One*, **8**, e73710.
14. Deraska,P.V., O'Leary,C., Reavis,H.D., Labe,S., Dinh,T.K., Lazaro,J.B., Sweeney,C., D'Andrea,A.D. and Kozono,D. (2018) NF-kappaB inhibition by dimethylaminoparthenolide radiosensitizes non-small-cell lung carcinoma by blocking DNA double-strand break repair. *Cell Death Discov.*, **4**, 10.
15. Volcic,M., Karl,S., Baumann,B., Salles,D., Daniel,P., Fulda,S. and Wiesmuller,L. (2012) NF-kappaB regulates DNA double-strand break repair in conjunction with BRCA1-CtIP complexes. *Nucleic Acids Res.*, **40**, 181–195.
16. Yarde,D.N., Oliveira,V., Mathews,L., Wang,X., Villagra,A., Boulware,D., Shain,K.H., Hazlehurst,L.A., Alsina,M., Chen,D.T. *et al.* (2009) Targeting the fanconi anemia/BRCA pathway circumvents drug resistance in multiple myeloma. *Cancer Res.*, **69**, 9367–9375.
17. Benezra,M., Chevallier,N., Morrison,D.J., MacLachlan,T.K., El-Deiry,W.S. and Licht,J.D. (2003) BRCA1 augments transcription by the NF-kappaB transcription factor by binding to the rel domain of the p65/RelA subunit. *J. Biol. Chem.*, **278**, 26333–26341.
18. Gilmore,T.D. and Herscovitch,M. (2006) Inhibitors of NF-kappaB signaling: 785 and counting. *Oncogene*, **25**, 6887–6899.
19. Xia,L., Tan,S., Zhou,Y., Lin,J., Wang,H., Oyang,L., Tian,Y., Liu,L., Su,M., Wang,H. *et al.* (2018) Role of the NFkappaB-signaling pathway in cancer. *Onco Targets Ther*, **11**, 2063–2073.
20. Anthony,N.G., Baiget,J., Berretta,G., Boyd,M., Breen,D., Edwards,J., Gamble,C., Gray,A.I., Harvey,A.L., Hatziieremia,S. *et al.* (2017) Inhibitory kappa b kinase alpha (IKKalpha) inhibitors that recapitulate their selectivity in cells against isoform-related biomarkers. *J. Med. Chem.*, **60**, 7043–7066.
21. Paul,A., Edwards,J., Pepper,C. and Mackay,S. (2018) Inhibitory-kappaB kinase (IKK) alpha and nuclear Factor-kappaB (NFkappaB)-Inducing kinase (NIK) as anti-cancer drug targets. *Cells*, **7**, 176.
22. Bakhoum,S.F., Ngo,B., Laughney,A.M., Cavallo,J.A., Murphy,C.J., Ly,P., Shah,P., Sriram,R.K., Watkins,T.B.K., Taunk,N.K. *et al.* (2018) Chromosomal instability drives metastasis through a cytosolic DNA response. *Nature*, **553**, 467–472.
23. Sau,A., Lau,R., Cabrita,M.A., Nolan,E., Crooks,P.A., Visvader,J.E. and Pratt,M.A. (2016) Persistent activation of NF-kappaB in BRCA1-Deficient mammary progenitors drives aberrant proliferation and accumulation of DNA damage. *Cell Stem Cell*, **19**, 52–65.
24. Benjamini,Y. and Hochberg,Y. (1995) Controlling the false discovery rate - a Practical and powerful approach to multiple testing. *J. R. Stat. Soc. B.*, **57**, 289–300.
25. Smyth,G.K. (2004) Linear models and empirical bayes methods for assessing differential expression in microarray experiments. *Stat. Appl. Genet. Mol. Biol.*, **3**, Article3.
26. Fusco,A.J., Savinova,O.V., Talwar,R., Kearns,J.D., Hoffmann,A. and Ghosh,G. (2008) Stabilization of RelB requires multidomain interactions with p100/p52. *J. Biol. Chem.*, **283**, 12324–12332.
27. Saxon,J.A., Yu,H., Polosukhin,V.V., Stathopoulos,G.T., Gleaves,L.A., McLoed,A.G., Massion,P.P., Yull,F.E., Zhao,Z. and Blackwell,T.S. (2018) p52 expression enhances lung cancer progression. *Sci. Rep.*, **8**, 6078.
28. Bishop,D.K. (1994) RecA homologs dmc1 and rad51 interact to form multiple nuclear complexes prior to meiotic chromosome synapsis. *Cell*, **79**, 1081–1092.
29. Pierce,A.J., Johnson,R.D., Thompson,L.H. and Jasin,M. (1999) XRCC3 promotes homology-directed repair of DNA damage in mammalian cells. *Genes Dev.*, **13**, 2633–2638.
30. Paques,F. and Haber,J.E. (1999) Multiple pathways of recombination induced by double-strand breaks in saccharomyces cerevisiae. *Microbiol. Mol. Biol. Rev.*, **63**, 349–404.
31. Symington,L.S. (2002) Role of RAD52 epistasis group genes in homologous recombination and double-strand break repair. *Microbiol. Mol. Biol. Rev.*, **66**, 630–670.
32. Bennardo,N., Cheng,A., Huang,N. and Stark,J.M. (2008) Alternative-NHEJ is a mechanistically distinct pathway of mammalian chromosome break repair. *PLos Genet.*, **4**, e1000110.
33. Budke,B., Logan,H.L., Kalin,J.H., Zelivianskaia,A.S., Cameron McGuire,W., Miller,L.L., Stark,J.M., Kozikowski,A.P., Bishop,D.K. and Connell,P.P. (2012) RI-1: a chemical inhibitor of RAD51 that disrupts homologous recombination in human cells. *Nucleic Acids Res.*, **40**, 7347–7357.
34. Mansour,W.Y., Schumacher,S., Rosskopf,R., Rhein,T., Schmidt-Petersen,F., Gatzemeier,F., Haag,F., Borgmann,K., Willers,H. and Dahm-Daphi,J. (2008) Hierarchy of nonhomologous end-joining, single-strand annealing and gene conversion at site-directed DNA double-strand breaks. *Nucleic Acids Res.*, **36**, 4088–4098.
35. Stark,J.M., Pierce,A.J., Oh,J., Pastink,A. and Jasin,M. (2004) Genetic steps of mammalian homologous repair with distinct mutagenic consequences. *Mol. Cell. Biol.*, **24**, 9305–9316.
36. Del Bino,G., Lassota,P. and Darzynkiewicz,Z. (1991) The S-phase cytotoxicity of camptothecin. *Exp. Cell. Res.*, **193**, 27–35.
37. Pommier,Y., Redon,C., Rao,V.A., Seiler,J.A., Sordet,O., Takemura,H., Antony,S., Meng,L., Liao,Z., Kohlhagen,G. *et al.* (2003) Repair of and checkpoint response to topoisomerase I-mediated DNA damage. *Mutat. Res.*, **532**, 173–203.
38. Maede,Y., Shimizu,H., Fukushima,T., Kogame,T., Nakamura,T., Miki,T., Takeda,S., Pommier,Y. and Murai,J. (2014) Differential and common DNA repair pathways for topoisomerase I- and II-targeted drugs in a genetic DT40 repair cell screen panel. *Mol. Cancer Ther.*, **13**, 214–220.
39. Harding,S.M., Benci,J.L., Irianto,J., Discher,D.E., Minn,A.J. and Greenberg,R.A. (2017) Mitotic progression following DNA damage enables pattern recognition within micronuclei. *Nature*, **548**, 466–470.
40. Pitroda,S.P., Bao,R., Andrade,J., Weichselbaum,R.R. and Connell,P.P. (2017) Low recombination proficiency score (RPS) predicts heightened sensitivity to DNA-Damaging chemotherapy in breast cancer. *Clin. Cancer Res.*, **23**, 4493–4500.
41. Kang,J., D'Andrea,A.D. and Kozono,D. (2012) A DNA repair pathway-focused score for prediction of outcomes in ovarian cancer treated with platinum-based chemotherapy. *J. Natl. Cancer Inst.*, **104**, 670–681.
42. Swisher,E.M., Taniguchi,T. and Karlan,B.Y. (2012) Molecular scores to predict ovarian cancer outcomes: a worthy goal, but not ready for prime time. *J. Natl. Cancer Inst.*, **104**, 642–645.
43. Ceccaldi,R., Liu,J.C., Amunugama,R., Hajdu,I., Primack,B., Petalcorin,M.I., O'Connor,K.W., Konstantinopoulos,P.A., Elledge,S.J., Boulton,S.J. *et al.* (2015) Homologous-recombination-deficient tumours are dependent on Poltheta-mediated repair. *Nature*, **518**, 258–262.
44. Chan,S.H., Yu,A.M. and McVey,M. (2010) Dual roles for DNA polymerase theta in alternative end-joining repair of double-strand breaks in drosophila. *PLoS Genet.*, **6**, e1001005.
45. Yu,A.M. and McVey,M. (2010) Synthesis-dependent microhomology-mediated end joining accounts for multiple types of repair junctions. *Nucleic Acids Res.*, **38**, 5706–5717.
46. Chen,R. and Wold,M.S. (2014) Replication protein A: single-stranded DNA's first responder: dynamic DNA-interactions allow replication protein a to direct single-strand DNA intermediates into different pathways for synthesis or repair. *Bioessays*, **36**, 1156–1161.
47. Wold,M.S. (1997) Replication protein A: a heterotrimeric, single-stranded DNA-binding protein required for eukaryotic DNA metabolism. *Annu. Rev. Biochem.*, **66**, 61–92.
48. Mason,A.C., Haring,S.J., Pryor,J.M., Staloch,C.A., Gan,T.F. and Wold,M.S. (2009) An alternative form of replication protein a prevents viral replication in vitro. *J. Biol. Chem.*, **284**, 5324–5331.
49. Kemp,M.G., Mason,A.C., Carreira,A., Reardon,J.T., Haring,S.J., Borgstahl,G.E., Kowalczykowski,S.C., Sancar,A. and Wold,M.S. (2010) An alternative form of replication protein a expressed in normal human tissues supports DNA repair. *J. Biol. Chem.*, **285**, 4788–4797.
50. Mason,A.C., Roy,R., Simmons,D.T. and Wold,M.S. (2010) Functions of alternative replication protein a in initiation and elongation. *Biochemistry*, **49**, 5919–5928.
51. Zhao,B., Barrera,L.A., Ersing,I., Willox,B., Schmidt,S.C., Greenfeld,H., Zhou,H., Mollo,S.B., Shi,T.T., Takasaki,K. *et al.*

(2014) The NF-kappaB genomic landscape in lymphoblastoid b cells. *Cell Rep.*, **8**, 1595–1606.
52. Hasselbach,L., Haase,S., Fischer,D., Kolberg,H.C. and Sturzbecher,H.W. (2005) Characterisation of the promoter region of the human DNA-repair gene rad51. *Eur. J. Gynaecol. Oncol.*, **26**, 589–598.
53. Bindra,R.S. and Glazer,P.M. (2007) Repression of RAD51 gene expression by E2F4/p130 complexes in hypoxia. *Oncogene*, **26**, 2048–2057.
54. Lim,C.A., Yao,F., Wong,J.J., George,J., Xu,H., Chiu,K.P., Sung,W.K., Lipovich,L., Vega,V.B., Chen,J. *et al.* (2007) Genome-wide mapping of RELA(p65) binding identifies E2F1 as a transcriptional activator recruited by NF-kappaB upon TLR4 activation. *Mol. Cell*, **27**, 622–635.
55. Sun,S.C. (2012) The noncanonical NF-kappaB pathway. *Immunol. Rev.*, **246**, 125–140.
56. Bours,V., Franzoso,G., Azarenko,V., Park,S., Kanno,T., Brown,K. and Siebenlist,U. (1993) The oncoprotein bcl-3 directly transactivates through kappa b motifs via association with DNA-binding p50B homodimers. *Cell*, **72**, 729–739.
57. Nolan,G.P., Fujita,T., Bhatia,K., Huppi,C., Liou,H.C., Scott,M.L. and Baltimore,D. (1993) The bcl-3 proto-oncogene encodes a nuclear i kappa B-like molecule that preferentially interacts with NF-kappa b p50 and p52 in a phosphorylation-dependent manner. *Mol. Cell. Biol.*, **13**, 3557–3566.
58. Wang,V.Y., Li,Y., Kim,D., Zhong,X., Du,Q., Ghassemian,M. and Ghosh,G. (2017) Bcl3 phosphorylation by akt, erk2, and IKK is required for its transcriptional activity. *Mol. Cell*, **67**, 484–497.
59. Xu,X., Li,Y., Bharath,S.R., Ozturk,M.B., Bowler,M.W., Loo,B.Z.L., Tergaonkar,V. and Song,H. (2018) Structural basis for reactivating the mutant TERT promoter by cooperative binding of p52 and ETS1. *Nat. Commun.*, **9**, 3183.
60. Ibrahim,Y.H., Garcia-Garcia,C., Serra,V., He,L., Torres-Lockhart,K., Prat,A., Anton,P., Cozar,P., Guzman,M., Grueso,J. *et al.* (2012) PI3K inhibition impairs BRCA1/2 expression and sensitizes BRCA-proficient triple-negative breast cancer to PARP inhibition. *Cancer Discov.*, **2**, 1036–1047.
61. Wilson,L.A., Yamamoto,H. and Singh,G. (2004) Role of the transcription factor ets-1 in cisplatin resistance. *Mol. Cancer Ther.*, **3**, 823–832.
62. Basak,S., Kim,H., Kearns,J.D., Tergaonkar,V., O'Dea,E., Werner,S.L., Benedict,C.A., Ware,C.F., Ghosh,G., Verma,I.M. *et al.* (2007) A fourth IkappaB protein within the NF-kappaB signaling module. *Cell*, **128**, 369–381.
63. Ishimaru,N., Kishimoto,H., Hayashi,Y. and Sprent,J. (2006) Regulation of naive t cell function by the NF-kappaB2 pathway. *Nat. Immunol.*, **7**, 763–772.
64. Dejardin,E. (2006) The alternative NF-kappaB pathway from biochemistry to biology: pitfalls and promises for future drug development. *Biochem. Pharmacol.*, **72**, 1161–1179.
65. Novack,D.V. (2011) Role of NF-kappaB in the skeleton. *Cell Res.*, **21**, 169–182.
66. Blaquiere,N., Castanedo,G.M., Burch,J.D., Berezhkovskiy,L.M., Brightbill,H., Brown,S., Chan,C., Chiang,P.C., Crawford,J.J., Dong,T. *et al.* (2018) Scaffold-hopping approach to discover potent, selective, and efficacious inhibitors of NF-kappaB inducing kinase. *J. Med. Chem.*, **61**, 6801–6813.
67. Castanedo,G.M., Blaquiere,N., Beresini,M., Bravo,B., Brightbill,H., Chen,J., Cui,H.F., Eigenbrot,C., Everett,C., Feng,J. *et al.* (2017) Structure-based design of tricyclic NF-kappaB inducing kinase (NIK) inhibitors that have high selectivity over phosphoinositide-3-kinase (PI3K). *J. Med. Chem.*, **60**, 627–640.